EXHIBIT F

Ito and Rubin, *Cell* 96: 529-539 (1999)

Cell, Vol. 96, 529–539, February 19, 1999, Copyright ©1999 by Cell Press

gigas, a *Drosophila* Homolog of Tuberous Sclerosis Gene Product-2, Regulates the Cell Cycle

Naoto Ito and Gerald M. Rubin*
Howard Hughes Medical Institute
and Department of Molecular and Cell Biology
University of California, Berkeley
Berkeley, California 94720-3200

Summary

Tuberous sclerosis complex (TSC) is an autosomal dominant disorder leading to the widespread development of benign tumors that often contain giant cells. We show that the *Drosophila* gene *gigas* encodes a homolog of *TSC2*, a gene mutated in half of TSC patients. Clones of *gigas* mutant cells induced in imaginal discs differentiate normally to produce adult structures. However, the cells in these clones are enlarged and repeat S phase without entering M phase. Our results suggest that the TSC disorder may result from an underlying defect in cell cycle control. We have also identified a *Drosophila* homolog of *TSC1*.

Introduction

Tuberous sclerosis complex (TSC) is an autosomal dominant disorder affecting 1 in 5800 individuals. TSC occurs in multiple organs, including the brain, eyes, skin, kidney, heart, lungs, and skeleton, and is characterized by the presence of benign tumor cells termed hamartomas. Hamartomas are a mass of disorganized but differentiated cells indigenous to the site. TSC hamartomas rarely progress to malignancy, but brain hamartomas frequently cause epilepsy, mental retardation, autism, or attention deficit–hyperactive disorder (Gomez, 1988, 1991). One of the notable features of TSC hamartomas is the presence of giant cells in the tumors (Johnson et al., 1991).

Linkage studies in families with TSC have established two TSC loci, *TSC1* and *TSC2* (Povey et al., 1994), each accounting for approximately 50% of cases. The *TSC1* gene encodes a novel protein, hamartin, that contains a single transmembrane domain and a large cytoplasmic tail with coiled-coil domains (van Slegtenhorst et al., 1997). The *TSC2* gene encodes a novel protein, tuberin, that contains a region of homology to the GTPase-activating protein (GAP) for the small-molecular-weight GTPase Rap1 (The European Chromosome 16 Tuberous Sclerosis Consortium, 1993).

Mutations in the *TSC1* and *TSC2* genes have been described in patients with tuberous sclerosis (Wilson et al., 1996; van Slegtenhorst et al., 1997). Moreover, loss of heterozygosity at the *TSC1* and *TSC2* loci has been demonstrated in TSC patient lesions as well as in sporadic tumors of non-TSC patients (Green et al., 1994; Henske et al., 1995; van Slegtenhorst et al., 1997). These results support a tumor suppressor function for both *TSC1* and *TSC2*. The mechanism by which the loss of hamartin or tuberin produces tumors is unknown. The clinical features of *TSC1* and *TSC2* disease are indistinguishable (Povey et al., 1994), suggesting that the two TSC proteins participate in the same biochemical process. Since TSC mutations seem to affect cell growth, TSC proteins might be involved in the regulation of the cell cycle.

The *Drosophila* eye is well suited to the study of the cell cycle. The *Drosophila* compound eye is composed of an orderly array of approximately 800 unit eyes, or ommatidia. Each ommatidium consists of 20 neuronal and nonneuronal cells. The eye develops from a columnar epithelium, the eye imaginal disc. During the third larval instar, differentiation initiates in the posterior region of the eye disc and progresses anteriorly as a wave marked by a depression in the apical surface of the epithelium called the morphogenetic furrow (MF). Ahead of the MF, cells are undifferentiated and progress through the cell cycle asynchronously. All cells become synchronized in G_1, beginning just anterior to the MF. Cells emerging from the posterior edge of MF either terminally differentiate or enter a final synchronous round of cell division before terminal differentiation. Thus, the eye disc provides a system where cell cycle progression during development can be directly visualized as a continuum from the anterior edge of the MF extending posteriorly (Ready et al., 1976; Thomas et al., 1994).

We have conducted a genetic screen to identify new lethal mutations that affect adult eye structure. From this screen, we isolated a group of mutations that produce enlarged cells in homozygous mutant clones. We show that these mutations are allelic to a previously known mutant, *gigas* (Ferrús and García-Bellido, 1976; Canal et al., 1994). Here, we report the cloning and characterization of the *gigas* gene. *gigas* encodes a protein homologous to human TSC2. We have also isolated a cDNA that encodes a protein homologous to human TSC1. Phenotypic analysis of *gigas* mutant clones demonstrates that *gigas* blocks rereplication of DNA or promotes mitosis during imaginal disc development.

Results

Isolation of *C1* Mutants

We used the FRT/FLP recombination system (Xu and Rubin, 1993) to screen the left arm of the third chromosome for mutations affecting eye development. We screened ~150,000 X-ray-mutagenized progeny for abnormal morphology in eye clones and isolated 20 complementation groups of lethal mutations (see Experimental Procedures). One of these groups (*C1*), comprised of eight alleles, is described here. These mutations produce enlarged cells in mutant clones in the eye and wing (see below).

Scanning electron micrographs illustrate the external structure of a normal adult eye and an eye containing mutant clones for $C1^{56}$ (Figures 1A and 1B). The other

*To whom correspondence should be addressed (e-mail: gerry@fruitfly.berkeley.edu).

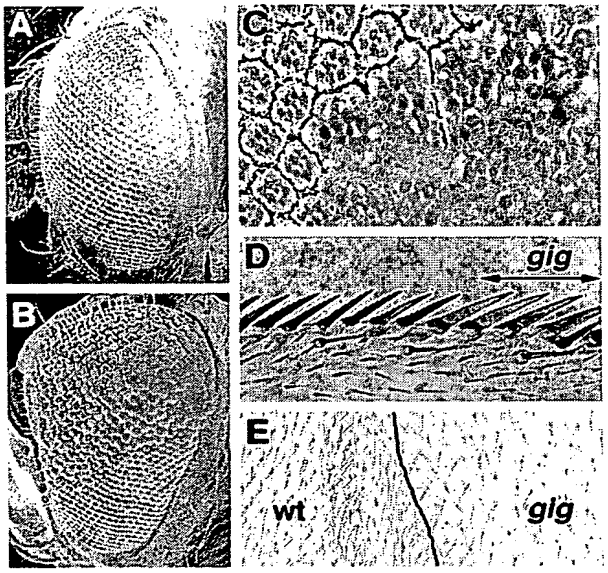

Figure 1. Adult Eye Phenotype of *gigas*

(A and B) Scanning electron micrographs of adult eyes are shown: (A) wild type (*w/y w* hsFLP122; P[ry$^+$; hs-neo; FRT]80B/*M(3)67C*; P[w$^+$; arm-lacZ]69C; P[ry$^+$; hs-neo; FRT]80B); (B) an eye carrying a clone of homozygous *gig*^{56} cells (*w/y w* hsFLP122; *gig*^{56}, P[ry$^+$; hs-neo; FRT]80B/*M(3)67C*; P[w$^+$; arm-lacZ]69C; P[ry$^+$; hs-neo; FRT]80B). Anterior is to the left.

(C) A phase contrast image of a section of *gig*^{62} clone in the adult eye. A mixture of pigmented wild-type and unpigmented *gigas* cells are shown. Note that cells in the *gig* mutant clone are enlarged and that the cell enlargement appears to be cell autonomous.

(D and E) Adult wings with *gig*^{62} mutant clones are shown. (D) Bristles at the anterior wing margin are shown. Note that *gigas* mutant bristles (yellowish color) are thicker and longer than the wild-type bristles, which are marked with *y*$^+$ and have a dark color. (E) A *gig*^{62} clone on the wing blade is shown. The clone of cells mutant for *gig* (indicated) is characterized by larger cell size and reduced cell density.

seven *C1* alleles display a similar eye phenotype. All unit eyes (ommatidia) in the mutant clone are two to three times larger in area than normal. Eye sections reveal that all the cells, including photoreceptor cells and non-neuronal accessory cells, are enlarged in the clone (Figure 1C); however, the structure and organization of ommatidia are nearly normal. Photoreceptors are occasionally missing, especially at clone borders where there are both normal and enlarged cells in the same ommatidia. Although *C1* mutant clones consist of larger cells, the developmental program of these cells seems to proceed normally. When mutant clones are generated in the wing, sensory bristles in the clones are larger but appear otherwise normal (Figure 1D). In *C1* clones on the wing blade, hair density is decreased (Figure 1F). Since all wing blade cells have a single hair at the same position, this result indicates that individual epidermal cells are larger. These results demonstrate that multiple cell types are affected by *C1*.

C1 Is Allelic to *gigas*

Recombination mapping placed the *C1* locus at 3-46 (cytological position 76-77), and deficiency mapping refined its position to 76F-77A2 (see Experimental Procedures). A previously described mutant, *gigas* (*gig*; meaning "giant" in Latin), exhibits a very similar large cell phenotype (Ferrús and García-Bellido, 1976; Canal et al., 1994). *gigas* was originally isolated as a mutant with larger bristles in clones (Ferrús and García-Bellido, 1976), and *gigas* mutant photoreceptors in eye clones are two to three times larger and establish more synapses than normal neurons (Canal et al., 1994). Although the reported map position of *gigas* (3-36.5; Canal et al., 1994) differed from that of *C1*, we found that all eight *C1* alleles failed to complement the three *gigas* alleles (*gig*^{109}, *gig*^{25}, and *gig*^{5C8}). This prompted us to remap *gigas*, and we found that its location did indeed coincide with that of *C1*. Since *C1* and *gigas* show similar phenotypes, fail to complement, and are at the same cytological location, we conclude that *C1* is allelic to *gigas* and henceforth refer to our *C1* mutations as *gigas* alleles.

Molecular Characterization of the *gigas* Locus

Individual BamHI and EcoRI fragments from a genomic P1 clone (DS01924) that covers the 76F-77A2 region were used to look for polymorphic DNA bands in genomic DNA blots of wild-type and *gigas* alleles. A 3.1 kb EcoRI fragment identified polymorphisms in BamHI–EcoRI double digests of two alleles, *gig*^{192} and *gig*^{193} (data not shown). No other EcoRI fragment revealed polymorphisms in the nine *gig* alleles tested. When this 3.1 kb fragment was used to screen a *Drosophila* embryo cDNA library, a single class of cDNAs was identified representing a transcript of 6.2 kb. Sequence analysis of the genomic region revealed that this transcript is encoded by 16 exons spanning 22 kb (Figure 2A).

We confirmed that this cDNA represents the *gigas* gene by determining that the open reading frame (ORF) it encodes is altered in *gigas* mutants and by showing that its ubiquitous expression was able to rescue the lethality of *gigas* mutations. The two strong alleles *gig*^{192} and *gig*^{193} were sequenced and found to contain small deletions within *gigas*-coding exons (see legend to Figure 2A). The *gig*^{192} mutation truncates the putative 1847 protein at amino acid 919, while *gig*^{193} deletes 56 amino acids (amino acids 472 to 527). Homozygous *gigas* animals are larval lethal and die by early third instar. Expression of the 6.2 kb full-length cDNA under the control of a heat shock promoter (*hs-gig*) using heat shock pulses at 12 hr intervals for 10 days completely rescued the lethality of three *gigas* alleles, *gig*^{56}, *gig*^{57}, and *gig*^{2253}. Adult flies from these rescue experiments are phenotypically normal. In two other *gig* alleles, *gig*^{193} and *gig*^{25}, larvae with the *hs-gig* transgene survive until late third instar, develop melanotic tumors (data not shown), and die at prepupal stage. Since the homozygous mutant animals die much earlier, we consider these to be partial rescue of *gigas* lethality. The strong *gigas* alleles (*gig*^{192} and *gig*^{273}) (see below) are not rescued, suggesting that the level of Gigas expression induced by twice daily heat shock pulses is not sufficient to rescue these alleles. Alternatively, the failure of complete rescue by this cDNA might be explained if alternative splicing generated additional protein forms. Nevertheless, we conclude that the transcript represented by this 6.2 kb cDNA corresponds to the *gigas* gene.

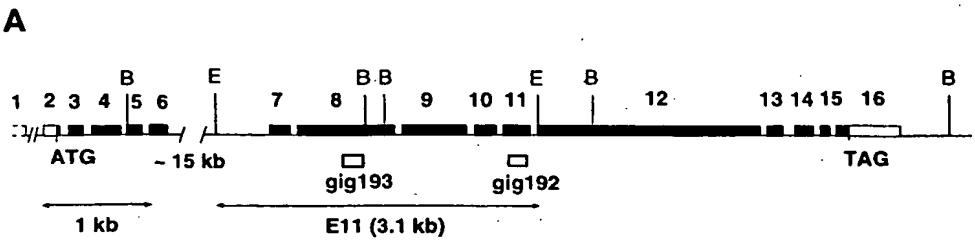

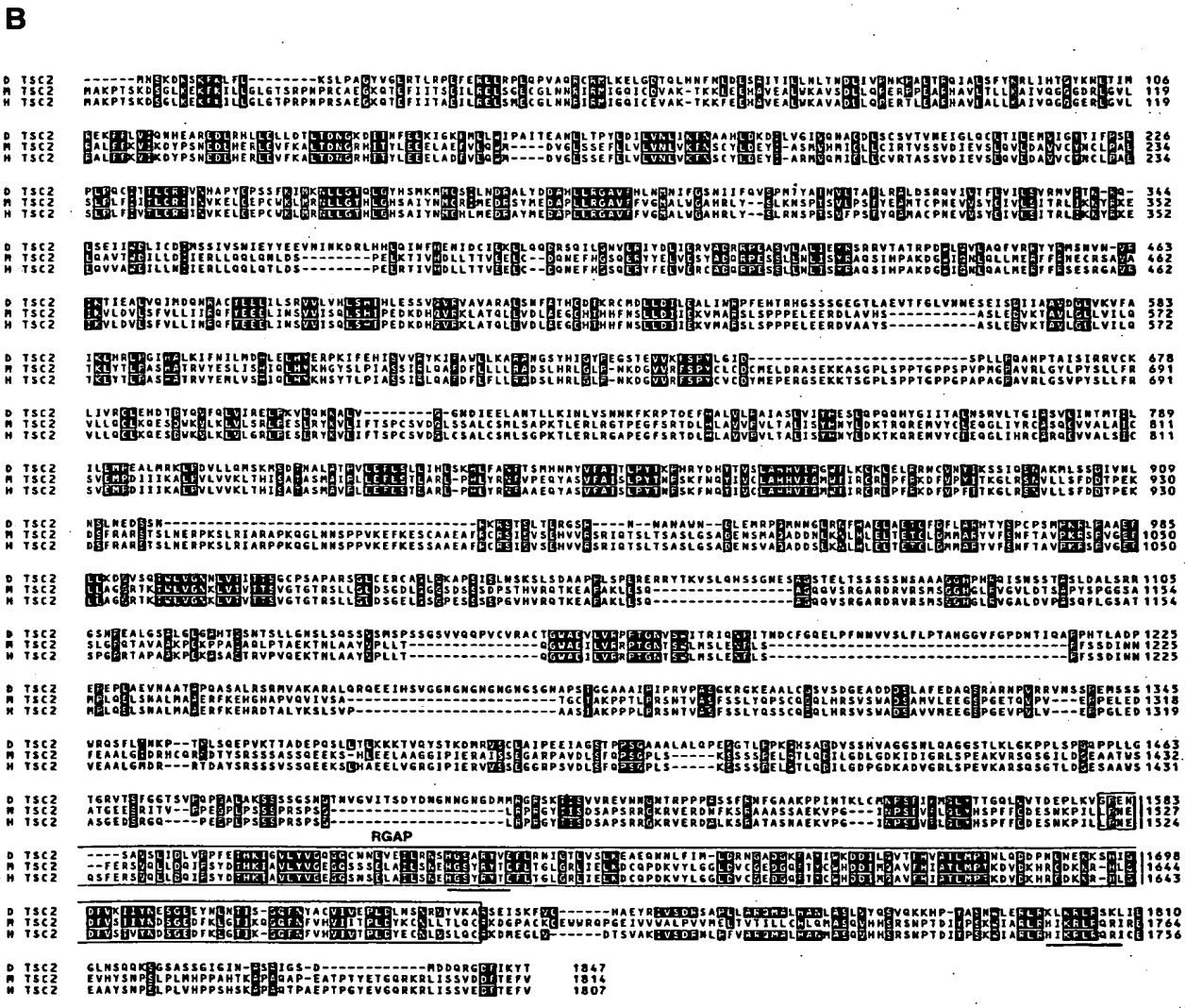

Figure 2. Molecular Characterization of the *gigas* Gene

(A) Map of the gigas genomic structure at 77A1-2. The boxes represent the 16 exons that comprise the gigas gene, with the closed boxes representing coding regions and the open boxes representing untranslated regions. Cleavage sites for BamHI (B) and EcoRI (E) are shown. The 3.1 kb EcoRI fragment (E11) that detected polymorphisms in two X-ray alleles, *gig*^{192} and *gig*^{193}, and the deletions found in these alleles are indicated. *gig*^{192} is a 161 bp deletion and 7 bp insertion that causes a frameshift after amino acid 919 and truncation of the protein after the addition of 16 out-of-frame amino acids. *gig*^{193} is a deletion of 166 bp and 10 bp insertion that causes an in-frame deletion of 56 amino acids from amino acids 472 to 527 and the addition of four amino acids. The centromere is to the right.

(B) An alignment of the amino acid sequences of TSC2/Gigas proteins from *D. melanogaster* (D TSC2), mouse (M TSC2; GenBank accession number U39818), and human (H TSC2; GenBank accession number P49815) produced using the CLUSTAL W program is shown. Residues identical to *Drosophila* are highlighted. The amino acid sequences homologous to Rap1GAP are boxed (RGAP). Potential GAP arginine fingers (Scheffzek et al., 1998) are underlined. The lack of sequence conservation with mouse between residues 1698–1728 is likely due to alternative splicing, as this region is encoded by a single exon in human (Maheshwar et al., 1996).

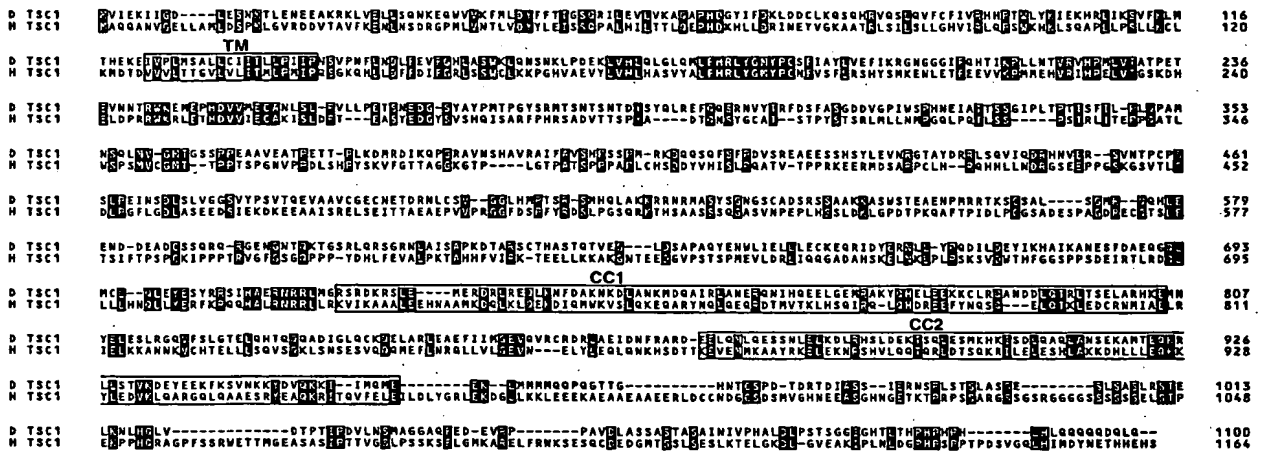

Figure 3. Sequence Comparison of the TSC1 proteins

Comparison of the amino acid sequences of TSC1 proteins from *D. melanogaster* (D TSC1) and human (H TSC1; GenBank accession number AF013168). The alignments were produced using the CLUSTAL W program as in Figure 2. A potential transmembrane domain (TM) and two potential coiled-coil domains (CC1 and CC2) are indicated.

The *gigas* Locus Encodes a *Drosophila* Homolog of Tuberous Sclerosis Gene TSC2

The *gigas* cDNA contains an ORF of 5541 bp, corresponding to a protein of 1847 amino acids. Searches of the current protein databases with this protein sequence indicate that the *gigas* gene encodes a *Drosophila* homolog of TSC2, or tuberin (The European Chromosome 16 Tuberous Sclerosis Consortium, 1993). No yeast or *C. elegans* homologs of either TSC1 or TSC2 were detected. Sequence alignment with the human and the mouse TSC2 proteins shows a high degree of conservation (Figure 2B). The human TSC2 protein is 26% identical (46% similar) to the Gigas protein.

The highest level of similarity (53% identity) is found in the 164 amino acids of the putative Rap1GAP domain (RGAP; Figure 2B). Recent reports indicate the presence of conserved arginine fingers in GAP proteins that are important for their catalytic activity (Scheffzek et al., 1998). TSC2/Gigas proteins have putative arginine fingers (Figure 2B, underlined) that do not resemble those of other known GAP subfamilies. Thus, TSC2 proteins might constitute a new subfamily of GAP proteins. Human TSC2 proteins were shown to have GAP activity in vitro for Rap1 (Wienecke et al., 1995) and Rab5 (Xiao et al., 1997), although the significance of these activities in vivo remains to be evaluated.

Isolation of the *Drosophila* TSC1 Homolog

Identification of the *Drosophila* TSC2 homolog prompted us to search for a *Drosophila* TSC1 homolog. We identified by BLAST search a *Drosophila* EST (LD11221; GenBank accession number AA392350) that displayed a significant similarity to the N-terminal sequence of human TSC1 (van Slegtenhorst et al., 1997). The sequence of the complete 3.8 kb cDNA predicts a protein of 1100 amino acids. Sequence alignment with the human TSC1 protein shows a significant degree of conservation (Figure 3). The human TSC1 protein is 22% identical (46% similar) to the *Drosophila* ORF. Furthermore, a single transmembrane domain is predicted for both human and *Drosophila* proteins at a conserved position, approximately 120 amino acids from the N terminus. A stretch of 133 amino acids in the potential cytoplasmic domain just after the transmembrane domain is highly conserved between human and *Drosophila* (44% identity). Coiled-coil domains, predicted for human, are found in similar positions in the *Drosophila* protein. Taken together with the overall level of protein sequence similarity, conservation of the transmembrane and coiled-coil domains strongly suggest that this cDNA encodes a *Drosophila* TSC1 homolog. We mapped this gene to 95E4-5 by in situ hybridization to polytene chromosomes.

Homozygous *gigas* Mutant Phenotypes

Homozygous *gigas* mutant larvae hatch normally but fail to survive beyond early third instar. To investigate whether a maternal contribution masks a requirement for *gigas* during embryonic development, we attempted to generate germline clones homozygous for *gigas*. We did not recover any eggs, however, indicating that Gigas is required for oogenesis and making it impossible to generate embryos totally lacking *gigas* product. Transheterozygotes of weak alleles often survive until late third instar, develop melanotic tumors, and die as prepupae. Melanotic tumors are black masses resulting from the melanization of hemocytes and are a frequent feature of the phenotype produced by various tumor suppressor mutants in *Drosophila* (reviewed in Gateff, 1994).

Cell Size Change of *gigas* Mutant Cells Occurs before Pattern Formation in the Eye Disc

To check when the cell size change occurs in *gigas* mutant clones, we used a *Minute* mutation, *M(3)67C*, to produce large mutant clones in the eye discs. *M(3)67C* is a loss-of-function mutation in the ribosomal protein *RPS17* (Maki et al., 1989). In mosaic discs, wild-type cells (M^+/M^+) grow faster and outcompete the M^+/M^-

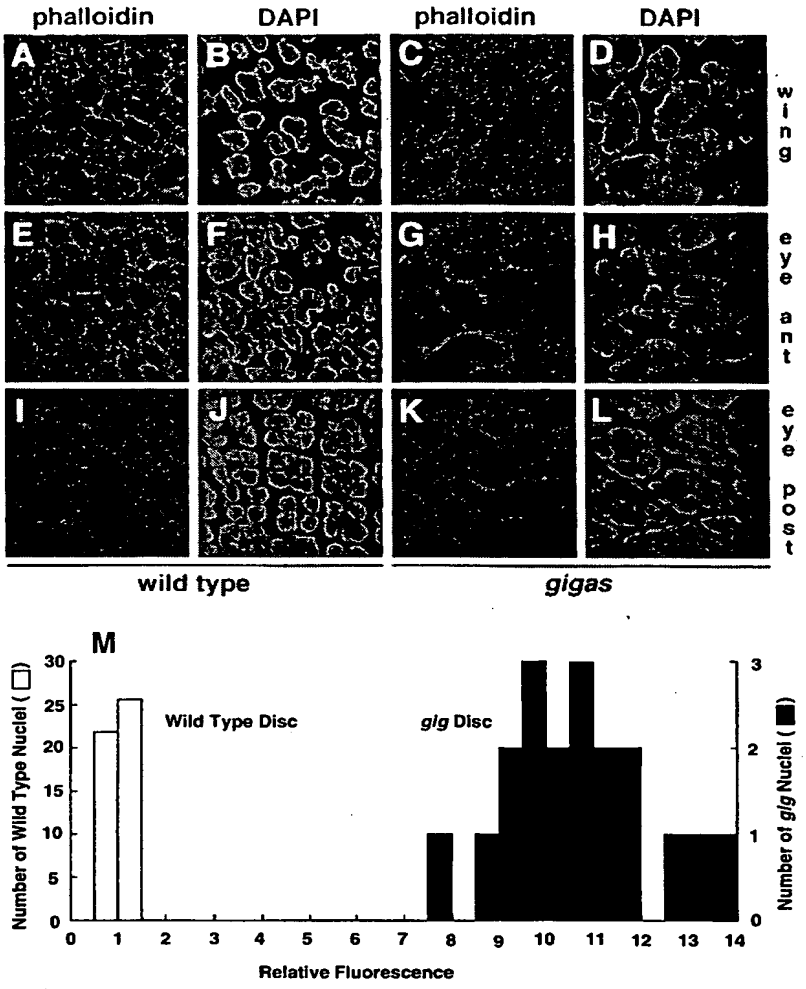

Figure 4. Enlarged Cells in *gigas* Clones in the Wing and Eye Imaginal Discs

(A–L) Confocal images of DNA-stained (DAPI; green) and phalloidin-stained (TRITC-phalloidin; red) wild-type (A, B, E, F, I, and J) and *gigas* (C, D, G, H, K, and L) cells are shown. (A–D), wing disc. (E–H), eye disc anterior to the morphogenetic furrow (MF). (I–L), eye disc posterior to the MF. Note the increased nuclear and cell size in cells mutant for *gigas*.

(M) Quantification of DNA content. DNA contents of wild-type and *gigas* cells in the wing discs were quantified from confocal images (see Experimental Procedures). The relative fluorescence values are shown with wild type assigned a value of 1.0. The 48 wild-type nuclei analyzed (open bars) had a mean value of 1.0 ± 0.2. In contrast, the 20 gig^{192} nuclei (closed bars) analyzed had a mean value of 10.6 ± 1.6.

cells to produce abnormally large clones (Simpson and Morata, 1981). Neither *M(3)67C* (data not shown) nor other *Minutes* (Neufeld et al., 1998a) alter cell size. Furthermore, cell cycle transitions occur at normal positions relative to the MF in the eye disc (Figures 6A, 6C, 7A, and 7D), and although tissue growth is slower in the M^+/M^- regions of the disc, cell cycle progression is still coordinately regulated (Figures 6A and 6C; Neufeld et al., 1998a).

To examine cell size and DNA content during development, we double-stained third instar imaginal discs containing *gigas* mutant clones with the DNA stain DAPI (4, 6-Diamidino-2-phenylindole) and the microfilament stain TRITC-phalloidin (Fen and Ready, 1997). Larger nuclei and increased cell sizes in the mutant clones were consistently observed. Examples taken from the wing and the eye disc are shown in Figures 4A–4L. This observation suggests that cell size has already increased in the developing imaginal discs. To measure the relative DNA content of *gigas* cells, the relative fluorescent intensity of DAPI-stained nuclei was measured from a series of confocal images (see Experimental Procedures). The average value obtained from wild-type wing disc cells was taken as 1.0. All the values from wild-type cells fell between 0.7–1.3 (1.0 ± 0.2). The mean value from *gig* cells was 10.6 ± 1.6 (Figure 4M), confirming that *gig* cells have endoreplicated without cell division.

Using the *Minute* mutation and heat shock–induced FLP, we can generate very large mutant clones that often encompass more than 90% of the discs. In M^-/M^+ larvae with large wild-type M^+/M^+ clones, imaginal discs are of normal size (data not shown). In the M^+, *gigas*/M^- larvae, discs with large *gigas* mutant clones (Figures 5C and 5D) are three to four times the size of wild-type discs in area (Figures 5A and 5B).

These results allow us to draw the following conclusions. First, cell size change in *gigas* clones is cell autonomous, since only the cells inside the clones are affected. Second, since many different kinds of cells in the eyes and wings are affected, it is likely that cell size change in mutant clones is due to a general defect in growth control rather than a defect in a particular developmental program. Third, cells anterior to the MF, which are unpatterned and undifferentiated, have large cell size, indicating that the effect of *gigas* mutations occurs before pattern formation and differentiation in eye discs.

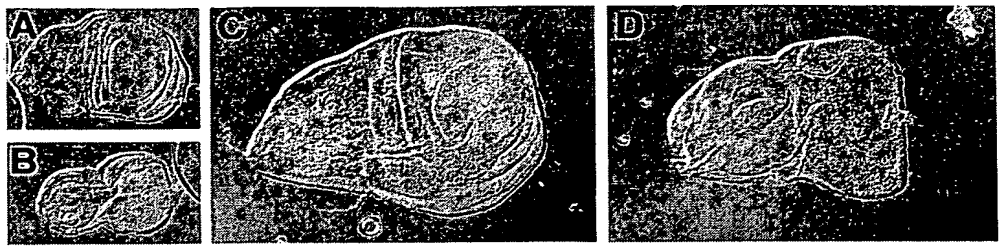

Figure 5. Increased Size of Wing and Eye Imaginal Discs that Carry Multiple *gigas* Clones

Phase contrast images of third instar imaginal discs are shown. (A) and (B) show wild-type wing (A) and eye (B) imaginal discs (genotype: *w/y w* hsFLP122; P[ry$^+$; hs-neo; FRT]80B/*M(3)67C*, P[w$^+$; arm-lacZ]69C; P[ry$^+$; hs-neo; FRT]80B). (C) and (D) show wing (C) and eye (D) imaginal discs in which multiple large *gigas* mutant clones have been induced (genotype: *w/y w* hsFLP122; *gig*^{192}, P[ry$^+$; hs-neo; FRT]80B/*M(3)67C*, P[w$^+$; arm-lacZ]69C). In (C) and (D), more than 90% of cells are mutant for *gigas*, and disc sizes are three to four times greater than in wild type at the same developmental stage. All the discs are shown at the same magnification.

Fourth, when clones occupy large areas of the discs, imaginal discs become enlarged, larval phase is extended, and animals die as prepupae.

gigas Mutant Cells Show Abnormal Cell Cycle Progression

We examined the pattern of cell cycle progression in the wild-type and *gigas* eye disc clones. First, we used the thymidine analog 5-bromo-2-deoxyuridine (BrdU) to label S phase cells. In a normal eye disc, many asynchronous S phase cells are seen in the region anterior to the MF, while cells enter S phase synchronously just posterior to the MF. In a wild-type eye disc, both anterior and posterior to the MF, many BrdU-positive cells are observed (Figure 6A). In a *gigas* mutant clone, the pattern of BrdU staining remains the same as wild type; however, fewer and larger BrdU-positive nuclei are observed (Figure 6B), which is consistent with the results seen with DAPI staining (Figure 4). These results clearly show that *gigas* mutant cells can still enter S phase and carry out DNA replication.

We next examined the distribution of M phase cells using an antibody specific for a phosphorylated form of histone H3 present only in mitotic nuclei (anti-PH3; Hendzel et al., 1997). In wild-type discs, M phase nuclei move to the apical surface of the disc (Wolff and Ready, 1993). Optical sections of a wild-type eye disc near the apical surface show that there are PH3-positive cells in regions both anterior and posterior to the MF (Figure 6C). In *gigas* mutant clones, no strong staining with anti-PH3 is seen either at the apical surface of the eye disc (Figure 6D) or in other regions of the eye discs (data not shown), implying that *gigas* mutant cells do not enter M phase in the developing eye discs.

These observations suggest that *gigas* mutant cells in the eye disc can still enter S phase but might not enter M phase. The fact that there are multiple cells in mutant clones, however, suggests that more than one type of cell cycle operates during the course of disc development and that Gigas is not required for all of the cell cycle types. Alternatively, Gigas might be a stable protein so that the phenotype is only manifested after several rounds of cell division.

We examined the expression of Elav, a nuclear protein expressed posterior to the furrow in differentiated neuronal cells (Figure 6E; Robinow and White, 1991). In a *gigas* clone (Figure 6F), the Elav-positive region in each cell is much larger than in wild type, reflecting larger nuclear size. However, the pattern of differentiation appears normal, again suggesting that pattern formation of mutant cells can proceed normally despite their cell cycle defect.

gigas Mutant Cells Accumulate G_2 Cyclins

To confirm that *gigas* mutant cells fail to enter M phase, we examined the expression patterns of the G_2 cyclins, Cyclin A and Cyclin B. In *Drosophila*, Cyclin A and Cyclin B have overlapping functions in regulating mitosis (Knoblich and Lehner, 1993). In a normal disc, the precursors to photoreceptors R8, R2, R5, R3, and R4 emerge from the MF, exit the mitotic cycle, and terminally differentiate. Other undifferentiated cells enter S phase and then G_2, where they accumulate Cyclin A and Cyclin B proteins in their cytoplasm. When G_2 cells enter M phase, Cyclin A and Cyclin B enter the nucleus and are degraded (Figures 7A and 7D; Thomas et al., 1997). After completing division, these cells differentiate to generate photoreceptors R1, R6, and R7, the primary, secondary, and tertiary pigment cells, the cone cells, and the bristle mother cells (Wolff and Ready, 1993). By contrast, in *gigas* mutant cells, cytoplasmic Cyclin A (Figures 7B and 7C) and Cyclin B (Figures 7E and 7F) remain at significant levels throughout the disc. Posterior to the MF in *gig* eye discs, the cells surrounding photoreceptor clusters express higher levels of Cyclin A and B (Figure 7). These are presumably pigment cells, cone cells, and the R1, R6, and R7 photoreceptor cells that go through an additional cell cycle. These cells still seem to respond to a developmental signal and upregulate G_2 cyclins, although the rapid downregulation of cyclins does not occur. Lower but significant levels of cyclins are detected in all other cells in the eye disc, including cells in the MF (Figure 7). These mutant cells are able to differentiate into the full range of cell types found in the adult eye despite their endoreplication phenotype.

Discussion

Gigas Is Required for the Decision Whether to Enter M Phase or S Phase

In this report, we show that *gigas* mutant cells endoreplicate their DNA during the late stages of imaginal disc

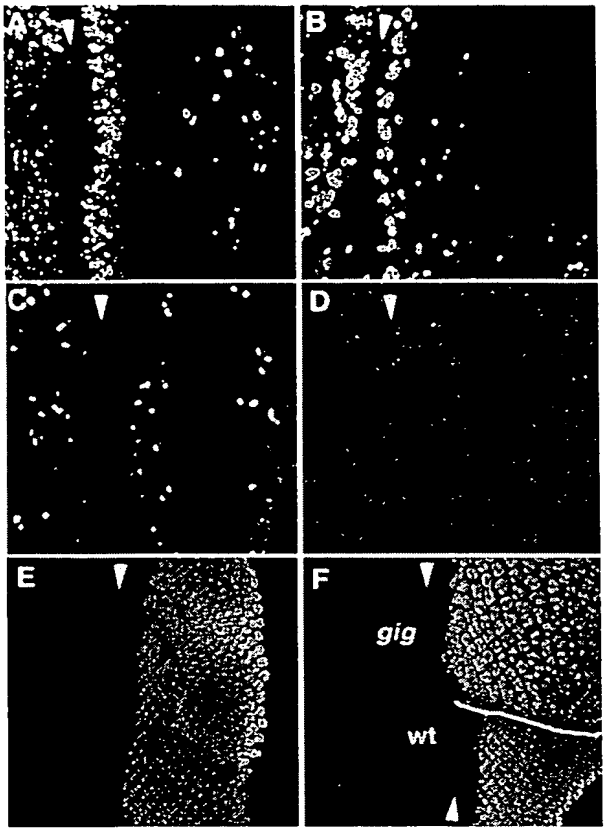

Figure 6. Inhibition of Cell Division and Normal DNA Replication Pattern in *gigas* Clones in Third Instar Eye Disc

Left panels (A, C, E) show confocal images of wild-type eye discs (genotype: *w/y w* hsFLP122; P[ry$^+$; hs-neo; FRT]80B/*M(3)67C*; P[w$^+$; arm-lacZ]69C; P[ry$^+$; hs-neo; FRT]80B). Right panels (B, D, F) show confocal images of eye discs with large *gig* clones (genotype: *w/y w* hsFLP122; *gig*^{192}, P[ry$^+$; hs-neo; FRT]80B/*M(3)67C*; P[w$^+$; arm-lacZ]69C; P[ry$^+$; hs-neo; FRT]80B). The position of the morphogenetic furrow (MF) is indicated by white arrowheads. (B) and (D) show only regions within *gigas* mutant clones. (F) shows both *gigas* mutant and wild-type regions, as indicated. (A and B) Third instar eye discs were incubated with BrdU in vitro, fixed, and analyzed. The anti-BrdU staining shows S phase cells both anterior and posterior to the MF. (C and D) Anti-phospho-histone H3 (M phase marker) staining of a wild-type eye disc (C) and of a *gigas* mutant clone in an eye disc (D). (E and F) Anti-Elav staining of a wild-type eye disc (E) and an eye disc with a *gigas* mutant clone (F). Anterior is to the left.

development. In normal cells, DNA replication is stringently regulated to guarantee that the genome is duplicated exactly once during each cell cycle. In *S. pombe*, the active mitotic cyclin-dependent kinase (CDK) activity (a complex of Cdc2 and its G2 cyclin partner Cdc13) is required for both mitosis and inhibition of the rereplication of DNA. Inhibition of the mitotic CDK activity by either inactivation of the Cdc2 itself, by inactivation of the cyclin Cdc13, or by overexpression of the Cdc2-Cyclin inhibitor Rum1 causes a block in mitosis and multiple rounds of DNA replication (Dahmann et al., 1995; Su et al., 1995; Stillman, 1996). In *Drosophila*, *cdc2* mutant cells rereplicate DNA without mitosis (Hayashi, 1996; Weigmann et al., 1997). These results suggest that the Cdc2-Cyclin complex is a crucial regulator of the decision whether to enter S phase or mitosis.

The effects of the *gigas* mutation could be explained by two possible mechanisms. First, Gigas may be required for blocking DNA rereplication. High levels of Cdc18 protein have been shown to inhibit mitosis and induce DNA rereplication in *S. pombe* (Stillman, 1996). Perhaps loss of Gigas function disrupts a similar control mechanism in *Drosophila*, resulting in an analogous endoreplication phenotype. Second, Gigas may be required for mitosis. In either case, the most probable target of Gigas activity is the Cdc2/Cyclin complex, a key regulator of mitosis. Cdc2 is maintained in an inactive phosphorylated form, and dephosphorylation of Cdc2 by the Cdc25 phosphatase leads to increased Cdc2 kinase activity and entry into mitosis (Morgan, 1997). If Gigas protein is required to activate the Cdc2 kinase, the *gigas* mutant phenotype may simply reflect the absence of active Cdc2. Alternatively, Gigas protein might regulate the subcellular localization of the Cdc2/Cyclin complex. The Cdc2/Cyclin complex accumulates in the cytoplasm during interphase but is imported into the nucleus at the start of M phase (Morgan, 1997). The accumulation of CycA and CycB in *gigas* mutant cells might be explained if the Gigas protein is required for nuclear import of Cdc2/Cyclin. The vertebrate TSC2 protein was reported to be localized to the Golgi/perinuclear region, consistent with a role in protein trafficking (Tsuchiya et al., 1996; Wienecke et al., 1996).

Since *gigas* mutant clones contain many cells, *gigas* mutant cells must initially be able to divide after mutant clones are produced by mitotic recombination. The explanation we favor to account for this ability is that there are multiple types of cell cycles and Gigas is only required for some of them. Previous results suggest that there are indeed different cell cycle types during imaginal disc development (Fain and Stevens, 1982; Kylsten and Saint, 1997). However, our data are also consistent with other explanations. For example, it is formally possible that Gigas protein is sufficiently stable that the phenotype is only manifested after several rounds of cell division following the generation of homozygous mutant cells.

A striking feature of the *gigas* mutant phenotype is the unusual accumulation of CycA and CycB. Sigrist et al. (1995) demonstrated that expression of mutant cyclins (A, B, or B3) lacking the destruction box motif blocked their degradation and arrested cells at metaphase or anaphase during embryonic development in *Drosophila*, indicating that exit from mitosis is regulated by destruction of G2 cyclins. In *gigas* mutant clones, cells repeat S phase without mitosis in the later phase of disc development. These results suggest that the failure to degrade CycA and CycB may be a consequence of the failure to enter M phase, rather than *gigas* mutants having a primary defect in cyclin degradation.

Cell Size and Disc Size Control

The increased cell size in adult mutant clones led to the initial identification of *gigas* (Ferrús and García-Bellido, 1976; this work). How cell size control and cell cycle are coupled is still not well understood. In general, the

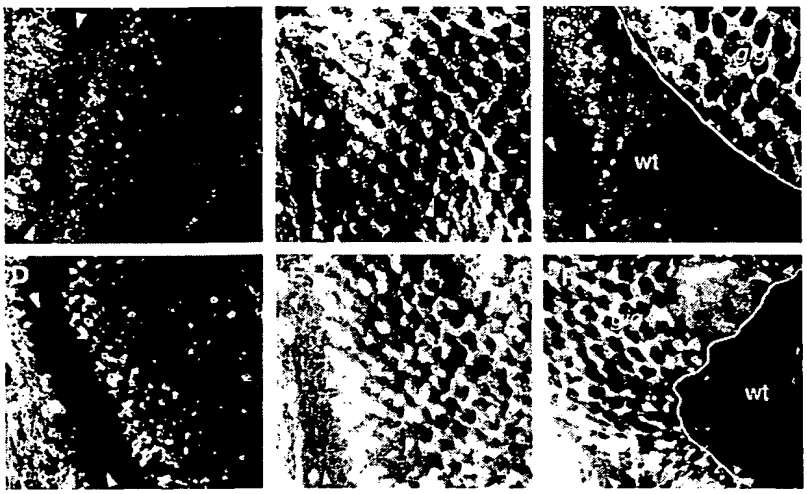

Figure 7. Accumulation of Cyclins A and B in *gig* Mutant Cells

Confocal images of wild-type eye discs (A and D) and eye discs with *gigas* mutant clones (B, C, E, and F) that were stained for anti-CycA (A–C) or anti-CycB (D–F) are shown. Genotypes of larvae are as described in Figure 6. In (B) and (E), the entire regions shown are within the *gigas* mutant clone. The position of the morphogenetic furrow (MF) is indicated with white arrowheads. In (C) and (F), the border between wild-type and *gigas* mutant tissue is indicated by a solid white line. In *gigas* mutant clones posterior to the MF, the cells expressing lower levels of cyclin proteins are surrounded by cells expressing higher levels of cyclin proteins in a regular pattern, each unit of which corresponds to an ommatidium. Anterior is to the left.

increase of cell size seems to correlate well with the increase of ploidy (Su and O'Farrell, 1998), suggesting that DNA replication may be coupled to cell growth. In *Drosophila* imaginal discs, inactivation of *cdc2* (Weigmann et al., 1997) or *gigas* leads to endoreplication and increased cell size. This common feature of the *gigas* and *cdc2* mutant phenotypes is consistent with a model that places Gigas and Cdc2/Cyclin in the same pathway of cell cycle control.

What makes an organ or a disc grow to a particular size is unknown. The loss of *cdc2* in wing discs results in discs of relatively normal size composed of fewer, larger cells, showing that even when cells are larger, disc size can still be regulated (Weigmann et al., 1997). In this report, we found that large *gigas* mutant clones that encompass more than 90% of the disc resulted in increased disc size three to four times larger than normal. We cannot distinguish at this time between two possible explanations for the difference between this aspect of the *gigas* and *cdc2* phenotypes. Gigas may be required for a cell size checkpoint. Thus, *gigas* mutant cells might not stop cell growth in response to signals controlling disc size, resulting in cell size continuing to increase to produce larger discs. Alternatively, the presence of significant numbers of wild-type cells in the same disc may result in signals that limit the cell size and thus disc size. Indeed, when only small *gigas* clones were created, disc size was close to normal (N. I. and G. M. R., unpublished). One possible explanation is that cell death in wild-type cells may be compensating for the overgrowth. It will be interesting to determine if creating large mutant clones of *cdc2* that encompass the entire disc produces larger discs.

Is TSC a Disease of Cell Cycle?

Studies of human TSC hamartomas noted the presence of giant cells (Johnson et al., 1991). TSC hamartomas are enlarged and disorganized while they express differentiation antigens specific to the site. Our observations with *gigas* mutant cells are consistent with these human phenotypes and suggest that the human TSC syndrome may also result from similar defects in cell cycle regulation. Benign TSC hamartomas might be the result of the endoreplication and cell size increase. The presence of *TSC1* and *TSC2* homologs in *Drosophila* strongly suggests the presence of the same cell cycle control mechanism in both human and *Drosophila*. Continued analysis of the *Drosophila TSC1* and *TSC2* genes should help achieve an understanding of the molecular mechanism of the TSC disease in humans.

Experimental Procedures

Fly Strains

The *y w* hsFLP122 strain was provided by Gary Struhl. Some of the original FRT lines for 3L chromosome (80-1, 80-w$^+$, 80-y$^+$; Xu and Rubin, 1993) were found to have an additional FRT at 73D in addition to the reported site at 80B. 80-πM (*w*; P[mini-w$^+$; hs-πM]75C, P[ry$^+$;hs-neo;FRT]80B) had only one FRT at 80B, and two new lines, each with a single FRT at 80B, were made from 80-πM for use in this study: 80-3 (*w*; P[ry$^+$;hs-neo;FRT]80B) and 80-3y$^+$ (*w*; P[ry$^+$; y$^+$]66E, P[w$^+$]70C, P[ry$^+$;hs-neo;FRT]80B).

The fly stocks *w*; P[w$^+$;arm-lacZ]69C and *w*; *M(3)67C*, P[mini-w$^+$; hs-πM]75C, P[ry$^+$;hs-neo;FRT]80B/TM6B were kindly provided by Jean-Paul Vincent and Mike Brodsky, respectively. The stocks *w*; P[w$^+$;arm-lacZ]69C, P[ry$^+$;hs-neo;FRT]80B and *w*; *M(3)67C*, P[w$^+$;arm-lacZ]69C/TM6B were generated by recombination. Two *gigas* EMS alleles (*gig*^{109} and *gig*^{25}) and one spontaneous allele (*gig*^{SC8}) (Canal et al., 1994) were kindly provided by Alberto Ferrús. *Df(3L)rdgC* (77A2;77E1) and *Df(3L)ri79C* (77B-C;77F-78A) were from the Bloomington Drosophila Stock Center.

Genetics

Fly culture and crosses were carried out according to standard procedures. The screen for mutant phenotypes in eye clones was carried out as described (Xu and Rubin, 1993). In brief, 80-1 (*w*; P[ry$^+$;hs-neo;FRT]73D, 80B) males were exposed to 4000 rad of X-rays and then mass mated with 80-w$^+$F (*y w* hsFLP1; P[w$^+$]70C, P[ry$^+$;hs-neo;FRT]73D, 80B) virgin females, eggs were collected for 24 hr, aged for another 24 hr, and heat-shocked in a 38°C water bath for 60 min. Approximately 150,000 F1 adults, of which 26,000 had *w* eye clones, were examined for a mutant phenotype in the *w* eye clones under a dissecting microscope. Putative mutants were crossed to *w*; TM3/TM6B flies and balanced lines were established. Progeny were crossed to 80-w$^+$F females and reconfirmed for the presence of mutations. A total of 93 mutants were recovered as balanced lines.

Complementation tests based on lethality were carried out between these lines. One of the complementation groups (*C1*) had eight alleles and was further characterized. One additional allele (*C1*^{2253}) was found among single P element insertion lines [l(3)02253;

Spradling et al., 1995], although C1 lethality was not associated with P insertion. *C1* alleles (*C1[55]*, *C1[56]*, *C1[57]*, *C1[62]*, *C1[192]*, *C1[193]*, *C1[201]*, *C1[273]*, *C1[2255]*) failed to complement preexisting *gigas* mutant alleles (*gig[109]*, *gig[25]*, and *gig[5C8]*) (Canal et al., 1994). *C1* and *gigas* were mapped meiotically with the markers *ru h th st cu sr e ca*. Approximately 200 potentially recombinant chromosomes were scored. *C1* and *gigas* lethalities were both mapped to 3-46.

The small deficiencies *XS572* (76B6;77C1), *XS533* (76B4;77B1), *XS411* (76C;77A), *XS2182* (76B;76F), and *XS705* (76B4;76D3) (Karim et al., 1996), *XS543* (76B;77A) (Neufeld et al., 1998b), *Df(3L)rdgC* (77A2;77E1), and *Df(3L)ri79C* (77B-C;77F-78A) were tested for failure to complement the lethality of *C1/gigas* mutants. Four of these deficiencies, *XS572*, *XS533*, *XS411*, and *XS543*, uncovered *C1/gigas* lethality.

Creation of mitotic clones was carried out as described (Xu and Rubin, 1993). Adult wings were dissected and mounted in Gary's magic mount (Basler and Struhl, 1994). To analyze clones in the imaginal discs, 80-3 (wild-type) or *w; gig*/TM6B males were mated to *y w* hsFLP122; *M(3)67C*, P[w+, arm-lacZ]69C, P[ry+; hs-neo; FRT]80B/TM6B virgin females and heat-shocked at 38°C as described above. Clones in the wing were identified with *y* marker (Xu and Rubin, 1993). Adult eye clones were identified using the *w* marker. Clones in the imaginal discs were identified using a ubiquitously expressed lacZ reporter (armadillo-lacZ; Vincent et al., 1994). Germline clones homozygous for *gigas* were generated using the dominant female sterile marker method (Chou et al., 1993) in *gig[192]*/P[ovo[D1]]3L females and *gig[56]*/P[ovo[D1]]3L females.

Isolation of Gigas Genomic DNA and cDNA

Genomic DNA was prepared from 80-1 and *w; gig*/TM6B lines and digested with a combination of two enzymes (BamHI–EcoRI, EcoRI–HindIII, or BamHI–HindIII), subjected to electrophoresis on 1% agarose gels, and transferred to Nylon membranes.

The genomic P1 clone DS01924 from 76F-77A2 (Kimmerly et al., 1996) was digested with BamHI or EcoRI and subcloned into pBluescript II (Stratagene). Individual fragments were tested for the ability to detect polymorphic DNA bands in genomic DNA blots of wild-type and *gigas* mutants. A 3.6 kb EcoRI fragment (E11; see Figure 2A) identified polymorphisms in *gig[192]* and *gig[193]* alleles. This fragment was used to screen ~400,000 pfu from a *Drosophila* embryo cDNA library in λzapII (LD library; Berkeley Drosophila Genome Project/HHMI EST Project, unpublished). We isolated 33 related cDNA clones of which the largest carried a 6.2 kb insert and was sequenced.

Isolation of *Drosophila TSC1* Homolog

We used the BLAST (Altschul et al., 1990) server at the Berkeley Drosophila Genome Project (http://www.fruitfly.org) to screen the Drosophila Expressed Sequenced Tag (EST) Database with the amino acid sequence of human *TSC1* (van Slegtenhorst et al., 1997). A *Drosophila* expressed sequence tag (EST clone number LD11221) that displayed significant similarity to the N-terminal sequence of *TSC1* was identified.

DNA Sequencing and Analysis

DNA sequences were performed by the dideoxy chain termination procedure (Sanger et al., 1977) using an ABI DNA sequencer. Templates were prepared by sonicating plasmid DNA and inserting the sonicated DNA into M13mp10 vector. The 6.2 kb *gigas* cDNA and 3.8 kb *Drosophila TSC1* cDNA (LD11221) were sequenced on both strands. The BLAST search program (Altschul et al., 1990; http://www.ncbi.nlm.nih.gov/BLAST) and the CLUSTAL W multiple sequence alignment program (Thompson et al., 1994; http://pbil.ibcp.fr/NPSA/npsa_clustalw.html) were used for sequence similarity analysis.

Rescue of *gigas* Lethality

In order to express the *gigas* cDNA under the heat shock promoter, the full-length *gigas* cDNA (6.2 kb) was inserted into the NotI site of pCaSpeR-hs (Pirrotta et al., 1988) and used to generate transgenic lines. Virgin females with two copies of transgene (hs-gig) on the second chromosome [*w*; pw+(hs-gig)/pw+(hs-gig); TM3/TM6B] were mated to *w; gig*/TM6B males. Virgin females and males carrying both the transgene and *gigas* mutation (*w*; hs-gig/+; *gig*/TM6B) were mated. Eggs were collected for 12 hr and heat-shocked every 12 hr for 10 days using 90 min incubations in a 37°C air incubator.

Scanning Electron Microscopy

Adult flies were prepared for scanning electron microscopy as described (Kimmel et al., 1990) except that hexamethyldisilazane (HMDS; Braet et al., 1997) was used instead of Freon. Briefly, adult flies were fixed and incubated in 25%, 50%, 75%, and 100% ethanol. Ethanol was then replaced by 100% HMDS and flies were dried under vacuum overnight.

Histology and Immunohistochemistry

Adult eyes were fixed, embedded, and sectioned as described (Tomlinson and Ready, 1987a). All the third instar larvae were collected at the wandering stage. Third instar eye imaginal discs were fixed and stained as described (Tomlinson and Ready, 1987b; Thomas et al., 1997). Monoclonal antibodies to CycA (A12) and CycB (F2F4) were a generous gift of P. O'Farrell. Rat anti-Elav monoclonal antibody was diluted 1:10. Rabbit anti-phospho-histone H3 (Upstate Biotechnology) was diluted 1:1000. Cy3-conjugated anti-rat and anti-mouse antibodies (Jackson) were used at a 1:400 dilution. Anti-CycA and anti-CycB antibody supernatants were diluted 1:200. For anti-CycA, anti-CycB, and anti–β galactosidase staining, the signal was amplified using ABC kit (Vector Laboratories) and Cy3-conjugated tyramide (TSA direct, NEN). For DNA staining and phalloidin staining, fixed discs were incubated with DAPI (1 μg/ml) and TRITC-phalloidin (Sigma; 1 μM). Discs were mounted in 90% glycerol in phosphate-buffered saline (PBS). Confocal microscopy was done using a Leica TCS NT microscope. Confocal images were pseudocolored and merged using Adobe Photoshop.

BrdU Labeling

BrdU in vitro labeling was done as described (Winberg et al., 1992) with minor modifications. Third instar larvae were dissected in PBS and eye discs were incubated in a 60 μg/ml solution of BrdU (Sigma) in PBS for 30 min at 25°C. Discs were fixed for 20 min in 4% paraformaldehyde, washed, and then treated with 3 M HCl for 30 min. After washing, discs were blocked in 0.1% Triton X-100/3% normal goat serum in PBS and stained with mouse anti-BrdU antibody (1:50; Becton-Dickinson) and Cy3-conjugated anti-mouse antibody as described above.

Image Analysis

Image analysis was performed using the public domain NIH Image program 1.61 (http://rsb.info.nih.gov/nih-image/). The DNA content of individual cells was quantified from confocal images of DAPI-stained cells using NIH Image. Briefly, third instar wing imaginal discs were fixed for 20 min in 4% paraformaldehyde, washed, and stained with DAPI (1 μg/ml) at 4°C overnight. The discs were washed and mounted in 90% glycerol in PBS. A z series of confocal images were acquired with a constant distance of 2/3 μm between slices. Images were acquired in a linear range of DAPI fluorescence. Four (wild-type nuclei) or six (*gig* nuclei) images were projected to a single plane using the mean value projection method, and the mean fluorescence value for each nucleus was measured. The resulting values were multiplied by the number of pixels in the region and the number of sections used to make a single projection.

Acknowledgments

We would like to thank H. Chang, B. Hay, T. Neufeld, I. Rebay, J. Treisman, T. Xu, and current members of the Rubin lab for useful discussion during this work. We especially thank P. O'Farrell for his critical comments. We thank I. Hariharan, A. Bailey, M. Brodsky, A. Huang, T. Kidd, A. Page-McCaw, and A. Tang for critical reading of the manuscript. We thank N. Wakabayashi-Ito for helpful comments and continuous encouragement. We thank T. Wolff for examining discs and eye sections. We also thank M. Brodsky, A. Ferrús, F. Karim, T. Neufeld, G. Struhl, and J.-P. Vincent for fly stocks, and B. J. Thomas for the disc staining protocol for anti-cyclin A and anti-cyclin B. We thank T. Laverty for analysis of polytene chromosomes and confocal microscopy; C. Suh and G. Tsang for DNA

sequencing; and A. Valeros and S. Mullaney for injection of embryos. We also thank H. Aaron, T. Brotz, R. Fetter, and C. Shatz for confocal microscopy and image analysis, and P. Sicurello for scanning electron microscopy. N. I. was supported by National Institutes of Health grant GM33135. G. M. R. is an Investigator of the Howard Hughes Medical Institute.

Received November 17, 1998; revised January 5, 1999.

References

Altschul, S.F., Gish, W., Miller, W., Myers, E.W., and Lipman, D.J. (1990). Basic local alignment search tool. J. Mol. Biol. *215*, 403–410.

Basler, K., and Struhl, G. (1994). Compartment boundaries and the control of Drosophila limb pattern by *hedgehog* protein. Nature *368*, 208–214.

Braet, F., De Zanger, R., and Wisse, E. (1997). Drying cells for SEM, AFM and TEM by hexamethyldisilazane: a study on hepatic endothelial cells. J. Microsc. *186*, 84–87.

Canal, I., Fariñas, I., Gho, M., and Ferrús, A. (1994). The presynaptic cell determines the number of synapses in the Drosophila optic ganglia. Eur. J. Neurosci. *6*, 1423–1431.

Chou, T.B., Noll, E., and Perrimon, N. (1993). Autosomal P[ovoD1] dominant female-sterile insertions in Drosophila and their use in generating germ line chimeras. Development *119*, 1359–1369.

Dahmann, C., Diffley, J.F.X., and Nasmyth, K.A. (1995). S-phase-promoting cyclin-dependent kinases prevent re-replication by inhibiting the transition of replication origins to a pre-replicative state. Curr. Biol. *5*, 1257–1269.

Fain, M.J., and Stevens, B. (1982). Alterations in the cell cycle of Drosophila imaginal disc cells precede metamophosis. Dev. Biol. *92*, 247–258.

Fen, S., and Ready, D.F. (1997). *Glued* participates in distinct microtubule-based activities in Drosophila eye development. Development *124*, 1497–1507.

Ferrús, A., and Garcia-Bellido, A. (1976). Morphogenetic mutants detected in mitotic recombination clones. Nature *260*, 425–426.

Gateff, E. (1994). Tumor suppressor and overgrowth suppressor genes of Drosophila melanogaster. Developmental aspects. Int. J. Dev. Biol. *38*, 565–590.

Gomez, M.R. (1988). Tuberous Sclerosis, Second Edition (New York: Raven Press).

Gomez, M.R. (1991). Phenotypes of the tuberous sclerosis complex with a revision of diagnostic criteria. Ann. N.Y. Acad. Sci. *615*, 1–7.

Green, A.J., Smith, M., and Yates, J.R.W. (1994). Loss of heterozygosity on chromosome 16p13.3 in hamartomas from tuberous sclerosis patients. Nat. Genet. *6*, 193–196.

Hayashi, S. (1996). A Cdc2 dependent checkpoint maintains diploidy in Drosophila. Development *122*, 1051–1058.

Hendzel, M.J., Wei, Y., Mancini, M.A., Van Hooser, A., Ranalli, T., Brinkley, B.R., Bazett-Jones, D.P., and Allis, C.D. (1997). Mitosis-specific phosphorylation of histone H3 initiates primarily within pericentromeric heterochromatin during G2 and spreads in an ordered fashion coincident with mitotic chromosome condensation. Chromosoma *106*, 348–360.

Henske, E.P., Neumann, H.P.H., Scheithauer, B.W., Herbst, E.W., Short, M.P., and Kwiatkowski, D.J. (1995). Loss of heterozygosity in the tuberous sclerosis (TSC2) region of chromosome band 16p13 occurs in sporadic as well as TSC-associated renal angiomyolipomas. Genes Chromosomes Cancer *13*, 295–298.

Johnson, W.G., Yoshidome, H., Sternroos, E.S., and Davidson, M.M. (1991). Origin of the neuron-like cells in tuberous sclerosis tissues. Ann. N.Y. Acad. Sci. *615*, 211–219.

Karim, F.D., Chang, H.C., Therrien, M., Wasserman, D.A., Laverty, T., and Rubin, G.M. (1996). A screen for genes that function downstream of *Ras1* during Drosophila eye development. Genetics *143*, 315–329.

Kimmel, B.E., Heberlein, U., and Rubin, G.M. (1990). The homeo domain protein *rough* is expressed in a subset of cells in the developing Drosophila eye where it can specify photoreceptor cell subtype. Genes Dev. *4*, 712–727.

Kimmerly, W., Stultz, K., Lewis, S., Lewis, K., Lustre, V., Romero, R., Benke, J., Sun, D., Shirley, G., Martin, C., and Palazzolo, M. (1996). A P1-based physical map of the Drosophila euchromatic genome. Genome Res. *6*, 414–430.

Knoblich, J.A., and Lehner, C.F. (1993). Synergistic action of Drosophila cyclins A and B during the G2-M transition. EMBO J. *12*, 65–74.

Kylsten, P., and Saint, R. (1997). Imaginal tissues of Drosophila melanogaster exhibit different modes of cell proliferation control. Dev. Biol. *192*, 509–522.

Maheshwar, M.M., Sandford, R., Nellist, M., Cheadle, J.P., Sgotto, B., Vaudin, M., and Sampson, J.R. (1996). Comparative analysis and genomic structure of the tuberous sclerosis 2 (TSC2) gene in human and pufferfish. Hum. Mol. Genet. *5*, 131–137.

Maki, C., Rhoads, D.D., Stewart, M.J., Van Slyke, B., and Roufa, D.J. (1989). The Drosophila melanogaster RPS17 gene encoding ribosomal protein S17. Gene *79*, 289–298.

Morgan, D.O. (1997). Cyclin-dependent kinases: engines, clocks, and microprocessors. Annu. Rev. Cell Dev. Biol. *13*, 261–291.

Neufeld, T.P., de la Cruz, A.F.A., Johnston, L.A., and Edgar, B.A. (1998a). Coordination of growth and cell division in the *Drosophila* wing. Cell *93*, 1183–1193.

Neufeld, T.P., Tang, A.H., and Rubin, G.M. (1998b). A genetic screen to identify components of the *sina* signaling pathway in Drosophila eye development. Genetics *148*, 277–286.

Pirrotta, V., Bickel, S., and Mariani, C. (1988). Developmental expression of the Drosophila *zeste* gene and localization of *zeste* protein on polytene chromosomes. Genes Dev. *2*, 1839–1850.

Povey, S., Burley, M.W., Attwood, J., Benham, F., Hunt, D., Jeremiah, S.J., Franklin, D., Gillet, G., Malas, S., Robson, E.B., et al. (1994). Two loci for tuberous sclerosis: one on 9q34 and one on 16p13. Ann. Hum. Genet. *58*, 107–127.

Ready, D.F., Hanson, T.E., and Benzer, S. (1976). Development of the Drosophila retina, a neurocrystalline lattice. Dev. Biol. *53*, 217–240.

Robinow, S., and White, K. (1991). Characterization and spatial distribution of the *ELAV* protein during Drosophila melanogaster development. J. Neurobiol. *22*, 443–461.

Sanger, F., Nicklen, S., and Coulson, A. (1977). DNA sequencing with chain terminating inhibitors. Proc. Natl. Acad. Sci. USA *74*, 5463–5467.

Scheffzek, K., Ahmadian, M.R., and Wittinghofer, A. (1998). GTPase-activating proteins: helping hands to complement an active site. Trends Biochem. Sci. *23*, 257–262.

Sigrist, S., Jacobs, H., Stratmann, R., and Lehner, C.F. (1995). Exit from mitosis is regulated by Drosophila *fizzy* and the sequential destruction of cyclins A, B, and B3. EMBO J. *14*, 4827–4838.

Simpson, P., and Morata, G. (1981). Differential mitotic rates and patterns of growth in compartments in the Drosophila wing. Dev. Biol. *85*, 299–308.

Spradling, A.C., Stern, D.M., Kiss, I., Laverty, T., and Rubin, G.M. (1995). Gene disruptions using P transposable elements: an integral component of the Drosophila genome project. Proc. Natl. Acad. Sci. USA *92*, 10824–10830.

Stillman, B. (1996). Cell cycle control of DNA replication. Science *274*, 1659–1664.

Su, T.T., and O'Farrell, P.H. (1998). Size control: cell proliferation does not equal growth. Curr. Biol. *8*, R687–R689.

Su, T.T., Follette, P.J., and O'Farrell, P.H. (1995). Qualifying for the license to replicate. Cell *81*, 825–828.

The European Chromosome 16 Tuberous Sclerosis Consortium. (1993). Identification and characterization of the tuberous sclerosis gene on chromosome 16. Cell *75*, 1305–1315.

Thomas, B.J., Gunning, D.A., Cho, J., and Zipursky, S.L. (1994). Cell cycle progression in the developing Drosophila eye: *roughex* encodes a novel protein required for the establishment of G1. Cell *77*, 1003–1014.

Thomas, B.J., Zavitz, K.H., Dong, X., Lane, M.E., Weigmann, K., Finley, R.L., Jr., Brent, R., Lehner, C.F., and Zipursky, S.L. (1997). *roughex* down-regulates G2 cyclins in G1. Genes Dev. *11*, 1289–1298.

Thompson, J.D., Higgins, D.G., and Gibson, T.J. (1994). CLUSTAL W: improving the sensitivity of progressive multiple sequence alignment through sequence weighting, position-specific gap penalties and weight matrix choice. Nucleic Acids Res. *22*, 4673–4680.

Tomlinson, A., and Ready, D.F. (1987a). Cell fate in the Drosophila ommatidium. Dev. Biol. *123*, 264–275.

Tomlinson, A., and Ready, D.F. (1987b). Neuronal differentiation in the Drosophila ommatidium. Dev. Biol. *120*, 366–376.

Tsuchiya, H., Orimoto, K., Kobayashi, T., and Hino, O. (1996). Presence of potent transcriptional activation domains in the predisposing tuberous sclerosis (TSC2) gene product of the Eker rat model. Cancer Res. *56*, 429–433.

van Slegtenhorst, M., de Hoogt, R., Hermans, C., Nellist, M., Janssen, B., Verhoef, S., Lindhout, D., van den Ouwerland, A., Halley, D., Young, J., et al. (1997). Identification of the tuberous sclerosis gene TSC1 on chromosome 9q34. Science *277*, 805–808.

Vincent, J.-P., Girdham, C.H., and O'Farrell, P.H. (1994). A cell-autonomous, ubiquitous marker for the analysis of Drosophila genetic mosaics. Dev. Biol. *164*, 328–331.

Weigmann, K., Cohen, S.M., and Lehner, C.F. (1997). Cell cycle progression, growth and patterning in imaginal discs despite inhibition of cell division after inactivation of Drosophila Cdc2 kinase. Development *124*, 3555–3563.

Wienecke, R., König, A., and DeClue, J.E. (1995). Identification of tuberin, the tuberous sclerosis-2 product. Tuberin possesses specific Rap1GAP activity. J. Biol. Chem. *270*, 16409–16414.

Wienecke, R., Maize, J.C., Jr., Shoarinejad, F., Vass, W.C., Reed, J., Bonifacino, J.S., Resau, J.H., de Gunzburg, J., Yeung, R.S., and DeClue, J.E. (1996). Co-localization of the TSC2 product tuberin with its target Rap1 in the Golgi apparatus. Oncogene *13*, 913–923.

Wilson, P.J., Ramesh, V., Kristiansen, A., Bove, C., Jozwiak, S., Kwiatkowski, D.J., Short, M.P., and Haines, J.L. (1996). Novel mutations detected in the TSC2 gene from both sporadic and familial TSC patients. Hum. Mol. Genet. *5*, 249–256.

Winberg, M.L., Perez, S.E., and Steller, H. (1992). Generation and early differentiation of glial cells in the first optic ganglion of Drosophila melanogaster. Development *115*, 903–911.

Wolff, T., and Ready, D.F. (1993). Pattern formation in the Drosophila retina. In The Development of Drosophila melanogaster, M. Bate and A.M. Arias, eds. (Cold Spring Harbor, NY: Cold Spring Harbor Press), pp. 1277–1325.

Xiao, G.-H., Shoarinejad, F., Jin, F., Golemis, E.A., and Yeung, R.S. (1997). The tuberous sclerosis 2 gene product, tuberin, functions as a Rab5 GTPase activating protein (GAP) in modulating endocytosis. J. Biol. Chem. *272*, 6097–6100.

Xu, T., and Rubin, G.M. (1993). Analysis of genetic mosaics in developing and adult Drosophila tissues. Development *117*, 1223–1237.